Experimental Screening of Porous Materials for High Pressure Gas Adsorption and Evaluation in Gas Separations: Application to MOFs (MIL-100 and CAU-10)

Andrew D. Wiersum,[†] Christophe Giovannangeli,[†] Dominique Vincent,[†] Emily Bloch,[†] Helge Reinsch,[‡] Norbert Stock,[‡] Ji Sun Lee,[§] Jong-San Chang,[§] and Philip L. Llewellyn*,[†]

[†]Laboratoire MADIREL, Aix-Marseille Université, CNRS UMR7246, Centre de St Jérôme, Avenue Escadrille Normandie-Niemen, Marseille 13397 cedex 20, France

[‡]Institut für Anorganische Chemie, Christian-Albrechts-Universität zu Kiel, Max-Eyth-Straße 2, D-24118 Kiel, Germany

[§]Research Group for Nanocatalyst, Biorefinery Research Center, Korea Research Institute of Chemical Technology (KRICT), P.O. Box 107, Yusung, Daejeon 305-600, Korea

Ⓢ *Supporting Information*

ABSTRACT: A high-throughput gas adsorption apparatus is presented for the evaluation of adsorbents of interest in gas storage and separation applications. This instrument is capable of measuring complete adsorption isotherms up to 40 bar on six samples in parallel using as little as 60 mg of material. Multiple adsorption cycles can be carried out and four gases can be used sequentially, giving as many as 24 adsorption isotherms in 24 h. The apparatus has been used to investigate the effect of metal center (MIL-100) and functional groups

(CAU-10) on the adsorption of N_2, CO_2, and light hydrocarbons on MOFs. This demonstrates how it can serve to evaluate sample quality and adsorption reversibility, to determine optimum activation conditions and to estimate separation properties. As such it is a useful tool for the screening of novel adsorbents for different applications in gas separation, providing significant time savings in identifying potentially interesting materials.

KEYWORDS: metal−organic framework, functionalization, gas adsorption, screening, high-throughput, CO_2 capture
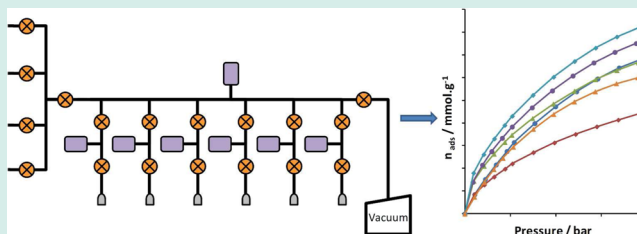
■ INTRODUCTION

The importance of porosity has long been recognized by scientists and engineers alike. As such, porous solids are widely encountered in industry and everyday life. In the domain of adsorption, porous solids can be found in processes such as ion exchange and the purification of liquids, as well as in gas separation and storage. Indeed, any separation step can constitute 50−80% of the capital expenditure of a chemical process. The interest of using an adsorption based process for separation lies in the fact that it is often a more economical than distillation or cryodistillation. Current examples of gas separation and storage include the recovery of carbon dioxide, the purification of hydrogen, and the separation of oxygen from air.[1,2] These examples emanate from current interests in the environmental and energy sectors. Here, techniques such as PSA (pressure swing adsorption) and TSA (temperature swing adsorption), are of interest in terms of rapidity, acceptable energy consumption, and minimal corrosion problems.[1] Even so, there is a continual search for more efficient porous materials. These can be novel materials with new structures and chemistries or materials that have been modified by ion exchange or other postsynthesis functionalization methods. Furthermore, the effect of different shaping protocols is equally

of interest to follow. In such cases and in a first instance, one may prepare small quantities of solid for an initial evaluation step prior to various levels of upscaling for the most promising materials. This is especially the case where high throughput synthesis methods are used for materials discovery and where milligram quantities of material are often prepared.

The evaluation of the porosity of these materials can be problematic. Indeed, most porous solids are characterized at 77 K using nitrogen as a probe. This method is not adapted for flexible materials, such as porous polymers or some metal−organic frameworks (MOFs), which can shrink at these low temperatures.[3] It is also not adapted for materials with small micropores, in the region of 0.4 nm.[4] Furthermore, as most applications occur at near ambient temperatures and most often with gases other than nitrogen, one should equally aim to characterize these solids with the relevant probe gas and ideally at near process conditions of temperature and pressure.

However, one problem arises in that many adsorption experiments at room temperature or above and up to high

pressures (>10 bar) require several hundred milligrams of sample to get reliable results, which is not practical for materials discovery. One would also like to obtain isotherms relatively rapidly and ideally test cycling conditions up to pressures of the process (i.e up to 30−40 bar in the case of CO_2 from natural gas, for example).

In terms of new materials, there is still much activity in the sector of metal−organic frameworks. These hybrid porous solids constitute a class of crystallized porous materials, which represent alternatives for many applications and are seen as a potential technological breakthrough. They combine inorganic and organic moieties which are built into 3D networks exclusively through strong bonds. Their advantage, compared to current materials, is that they can be built with almost any element of the periodic table. Consequently, they offer an almost infinite range of tunable chemistry, pore sizes and specific surface areas. High-throughput synthesis and characterization (notably XRD) methods are being used to discover new MOFs.[5,6] This in turn leads to the challenge to rapidly evaluate these porous properties and predict their separation behavior.

This initial evaluation screening step of the adsorption/ separation properties is very much in its infancy. Most commercially available multisample adsorption instruments focus on porosity and surface characterization, using adsorbates and conditions not always relevant to industrial processes.[7−9] The ASAP 2420 from Micromeritics[7] and the Autosorb-6B from Quantachrome[8] for example have principally been designed to measure the adsorption of gases such as nitrogen and argon at 77 or 87 K for BET type analyses. While they can also be used with other gases to screen materials for specific applications such as hydrogen storage,[10] they are limited to experiments up to atmospheric pressure. The InfraSORB developed by Wollmann et al.[9] is capable of analyzing twelve samples simultaneously and uses heat detection to investigate adsorption of n-butane and from that extrapolate properties, such as surface area and porosity. More recently, Han et al[11] developed an instrument to measure adsorption/desorption cycles on multiple samples in parallel to investigate their stability toward water vapor and acid gases such as SO_2 and NO_2. Their high-throughput approach involves measuring adsorption of relevant gases for flue gas separation at a single pressure value before and after exposure to the acid gases. As well as evaluating the stability of the adsorbents, because the pressure point selected is in the Henry's regime they are able calculate Henry's constants for each gas and estimate selectivity. This type of screening is important because the adsorbates (N_2, CO_2) and conditions (30 °C, 0−1 bar) used are directly relevant for the process being investigated. A potential limitation however of only measuring adsorption at a single pressure value arises when that value is no longer in the Henry's regime, as a more complete description of the isotherm is then required to determine selectivity.

Another possibility is to carry out screening of adsorbents using computer modeling. As well as providing insights into the adsorption mechanisms, molecular simulations using grand canonical Monte Carlo (GCMC), molecular dynamics (MD), and density functional theory (DFT) have shown to be able to predict with a reasonable degree of accuracy macroscopic phenomena, such as adsorption isotherms, heats of adsorption, and diffusion properties of gases in various adsorbents.[12,13] These tools have been used to evaluate and compare the adsorption and separation performances of a wide variety of materials including zeolites,[14−16] MOFs,[14,17] and ZIFs.[14,16] The advantage of using molecular simulations in screening is the possibility to investigate thousands of hypothetical materials as demonstrated in the studies of Kim et al.[15] and Lin et al.;[16] however there is no guarantee that these materials will one day be synthesized. In addition, it should be noted that in computational screening adsorbents are generally considered to be perfect models of the material, while the as-synthesized materials often present imperfections, which can substantially modify their performance.

The present contribution highlights the possibilities to screen porous materials for their potential use in gas storage or separation and several points are explored. Materials obtained from novel syntheses are often only available in small quantities and the possibility to screen mg quantities is of importance. Once materials of interest have been highlighted, the optimal thermal activation conditions may need to be determined to give the greatest adsorption capacity. The ability to sequentially measure isotherms with different gases can be of interest as long as each desorption step is fully reversible. The isotherms thus obtained with various gases can be fitted with classical isotherm models with further predictive models used to calculate selectivities. Equally of interest, cycling measurements can be performed to estimate the regenerability or stability of the adsorbent materials. The possibility to carry out experiments at different temperatures allows the estimation of isosteric heats of adsorption. The uptakes, calculated selectivities and isosteric heats can be used to compare between different solids, for example in the form of the "adsorbent performance indicator"[18] to highlight the materials of most potential interest.

■ EXPERIMENTAL SECTION

Samples. Two series of MOF samples have been used in this initial evaluation. The MIL-100(M) (MIL= material from the Institut Lavoisier) samples are a well-known and widely studied series of isostructural MOFs that can be synthesized with different metals.[19] The structure consists of two types of mesoporous cages approximately 25 and 29 Å in diameter, accessible through windows of approximately 5 and 9 Å. For some of the MIL-100 solids, there are multiple synthesize routes and in particular the presence or absence of HF in the recipe can impact the solid's properties.

The recently published CAU-10 MOF[20] (CAU = Christian Albrechts University) is made up of helical chains of cis-connected, corner sharing AlO_6-polyhedra linked by the V-shaped 1,3-benzene dicarboxylic acid or isophtalic acid to form square channels with a maximum diameter of 7 Å. This material has also successfully been synthesized using a variety of functionalized linkers to give the series of CAU-10-X solids, where X denotes the functional group (−CH_3, −OCH_3, −OH, −NH_2, −NO_2) in the 5-position on the aromatic ring. Narrow "openings" along the channels are formed by the aromatic rings of the linker and these range from 4 Å for the unmodified solid to 1.4 Å for the −CH_3-functionalized solid. Small variations in the framework structure have been observed, however, the topology of all the materials is the same.

The MOF samples were kindly provided by Prof. Chang from the Korea Research Institute of Chemical Technology (KRICT) in Daejeon and Prof. Stock from the Christian Albrechts University in Kiel. Full details for the synthesis of the functionalized CAU-10 samples have recently been published,[20] while details of the syntheses of the MIL-100 samples with different metals can be found in the Supporting Information.

112

dx.doi.org/10.1021/co300128w | ACS Comb. Sci. 2013, 15, 111−119

Table 1. Materials Investigated in this Study along with Their Characteristics (BET Surface Area and Pore Volume)

name	origin	BET surface area ($m^2 \cdot g^{-1}$)	pore volume ($cm^3_{liq} \cdot g^{-1}$)	reference
Takeda 5A	Takeda	1180	0.46	
MIL-100(Fe)_F1	KRICT	2190	0.85	21
MIL-100(Fe)_F2	KRICT	2400	0.99	21
MIL-100(Fe)_NF	KRICT	2260	0.88	22
MIL-100(Al)	KRICT	2034	0.76	23
MIL-100(Al)	Kiel	1932	0.77	23
MIL-100(Cr)	KRICT	2090	0.81	19
MIL-100(V)_1	KRICT	2170	0.84	24
MIL-100(V)_2	KRICT	2318	0.87	24
CAU-10-H	Kiel	635	0.25	20
CAU-10-OH	Kiel	no adsorption at 77 K		20
CAU-10-NH$_2$	Kiel	no measurement possible		20
CAU-10-NO$_2$	Kiel	410	0.19	20
CAU-10-OCH$_3$	Kiel	no measurement possible		20
CAU-10-CH$_3$	Kiel	no adsorption at 77 K		20

An activated carbon obtained from Takeda was equally investigated. The main characteristics of these samples are given in Table 1.
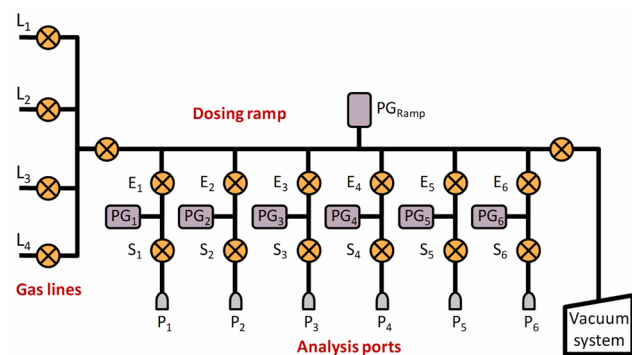

Figure 1. Schematic diagram of the high throughput apparatus used in this work.

Apparatus. The experimental setup was designed and constructed in house and is schematized in Figure 1. The system is constructed with Swagelok VCR 1/4 in. components with a series of pneumatic valves. Four gas lines are available that allow the sequential adsorption of gases as long as each individual isotherm is reversible under vacuum. Six samples can be analyzed almost in parallel. The ramp is used to increment doses for each individual reference volume (between valves E_x and S_x, volume ~5 cm^3). Each reference volume has its own pressure gauge PG_x (Mensor CPT6000 series, P_{max} = 40 bar), which means that the sample ports are completely independent from one another. This allows the possibility for both dosing to the sample and sample equilibrium to occur in parallel.

Gas adsorption is measured using a standard manometric technique, where gas is introduced stepwise into a reference volume (between E_x and S_x) before being brought into contact with the adsorbent by opening S_x. The amounts of gas adsorbed are calculated from the mass balance, using the Reference Fluid Thermodynamic and Transport Properties (REFPROP) software package 8.0 of the National Institute of Standards and Technology (NIST) by way of an equation of state.[25]

The system is set up so that each sample can be activated individually with its own heating mantle to a given final temperature under vacuum. During the adsorption experiments, the samples are placed in individual sand baths which are temperature controlled via a liquid thermostat (Julabo F25 ME = ± 0.01 °C) which can operated at −15 < T/°C < 120.
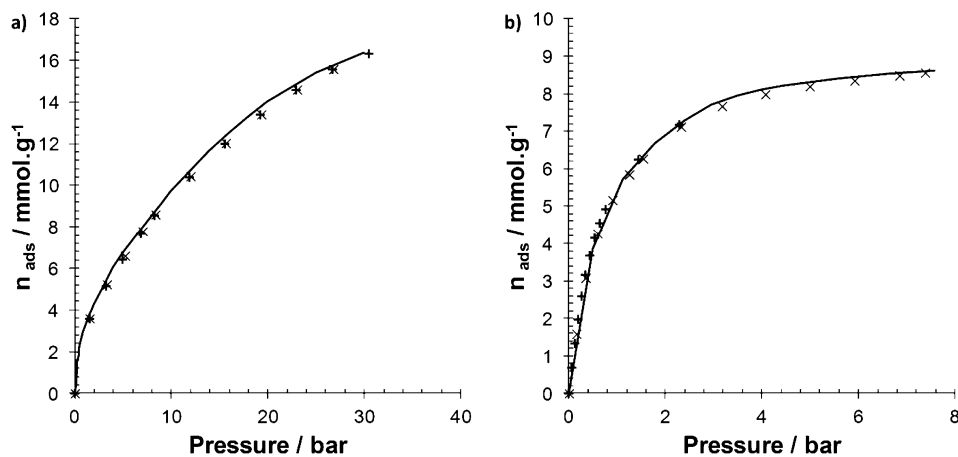

Figure 2. Adsorption isotherms for carbon dioxide on MIL-100(Fe)_F2 (a) and propylene on MIL-100(Al) (b) measured at 30 °C using the current apparatus and a magnetic suspension balance. ×, high-throughput apparatus cycle 1; +, high throughput apparatus cycle 2; solid line, magnetic suspension balance.
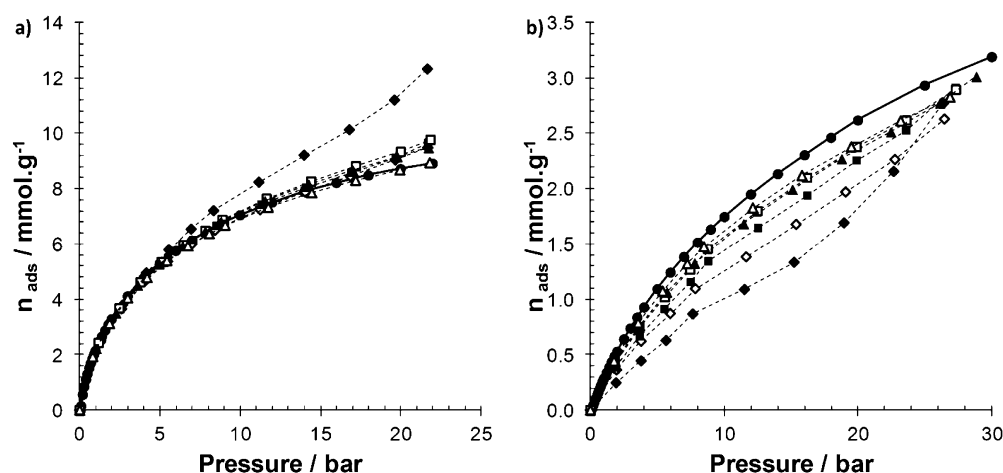
Figure 3. Adsorption isotherms for carbon dioxide (a) and nitrogen (b) on Takeda-5A measured at 30 °C using the apparatus with different amounts of adsorbent (♦, 15 mg; ◇, 25 mg; ■, 40 mg; □, 60 mg; ▲, 80 mg; △, 150 mg) and a magnetic suspension balance with 1 g (●).

It is possible to program multiple adsorption experiments with the same gas in order to follow reversibility on cycling with vacuum steps between each cycle. It is further possible to put the samples under vacuum, flush the lines with further gases allowing experiments with up to all of the four gases attached to the system. For ease of use, each isotherm is programmed with fixed equilibrium times and as such verifications should be made to ensure that equilibrium has been reached. Two dosing domains can be programmed to allow a concentration of equilibrium points if required; for example, during the initial loading. A typical adsorption experiment gives an isotherm with ten to fifteen measurement points for each sample and takes between 6 and 12 h.

The samples were outgassed under vacuum to specific final temperatures (see Table 1 in Supporting Information) for 16 h. A first series of experiments were carried out with gases which were shown to desorb fully under vacuum: He (for calibration), N_2, CH_4, and CO_2. The experiments with propane and propene were programmed individually with a thermal activation step between each gas. All experiments were cycled twice with a 2 h vacuum step between cycles. The gases were obtained from Air Liquide. Nitrogen and methane were of 99.9995% purity (N55), and carbon dioxide was 99.998% purity (N48), whereas propane and propene were of 99.95% purity (N35) or higher.

■ RESULTS AND DISCUSSION

Validation of Results Obtained with the Experimental Setup. Initial tests were carried out on the new apparatus to ensure that the results obtained are reliable and reproducible. Figure 2 compares two adsorption isotherms for CO_2 on MIL-100(Fe)_F2 (a) and C_3H_6 on MIL-100(Al) (b) measured using the new high-throughput apparatus on approximately 80 mg of sample with isotherms obtained with a commercial Rubotherm adsorption balance using approximately 1 g of sample (see Supporting Information for more details).

From these, it is possible to conclude first that the results are completely reproducible, even when varying the dose size to get more data in the low pressure region; second that the regeneration process (two hours under vacuum) is generally sufficient to remove all the adsorbed gas; and third that the results obtained with the new apparatus are in very good agreement with highly reliable gravimetric measurements using a much larger quantity of sample. Similar tests have been

carried out for N_2, CH_4, C_2H_6, and C_3H_8 with equally good results (see Supporting Information). In addition, the effect of varying the equilibrium times was investigated (see Supporting Information), indicating that the amount of time programmed (20−60 min depending on adsorbent and gas) is sufficient for the system to reach equilibrium.

Errors, Uncertainties, and Minimum Amount of Adsorbent. One of the main goals of this instrument being the evaluation of new adsorbents available in limited quantities, it is interesting to determine the minimum amount of sample required to get sufficiently accurate data for a screening step. "Sufficiently accurate" was arbitrarily set at ≤10% error compared to the gravimetric experiment at 20 bar. Adsorption isotherms of a strongly adsorbed gas (CO_2) and a weakly adsorbed gas (N_2) were measured on the commercial carbon molecular sieve (CMS) Takeda-5A with decreasing amounts of adsorbent from 150 to 15 mg and compared with the reference isotherm (denoted "Balance") obtained gravimetrically using approximately 1 g of material (see Figure 3).

As expected, the spread observed for the different amounts of adsorbent was much greater for the less-adsorbed nitrogen than for carbon dioxide. In terms of the acceptability criterion defined above, all the CO_2 measurements with the exception of the isotherm measured on 15 mg meet the required level of accuracy, while the isotherm measured on 150 mg of adsorbent is even accurate to within 2% over the whole pressure range investigated. Regarding nitrogen, 60 mg of Takeda-5A is the lowest amount that gives an isotherm deemed "acceptable", however, 40 mg is still accurate to within 15% and even the isotherm measured on 25 mg has the correct shape and gives a good idea of the order of magnitude of the amount adsorbed.

In addition to the comparison with the reference isotherm obtained gravimetrically, a detailed uncertainty analysis has been carried out based on the GUM (guide to the expression of uncertainty in measurements) method laid out by the International Organization for Standardization (ISO).[26] On the basis of these calculations, the absolute uncertainty in the amount adsorbed for each successive measurement point of the isotherm is approximately 5 μmol regardless of the gas used, the pressure in the system, the size of the injection and the amount adsorbed. The relative uncertainty however varies greatly depending on the amount of gas adsorbed, which is related not only to the mass of adsorbent but also to the gas. It follows
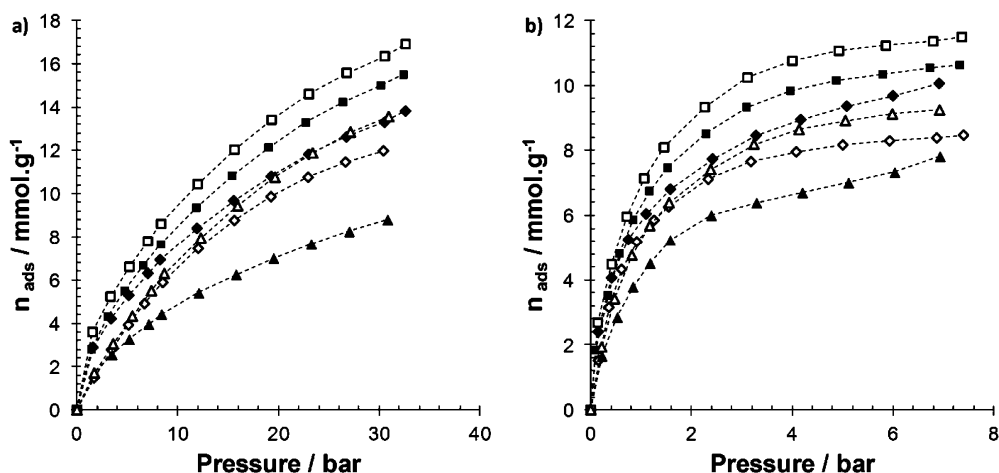
Figure 4. Adsorption isotherms for carbon dioxide (a) and propylene (b) on various MIL-100 materials measured at 30 °C. ♦, MIL-100(Cr); ◇, MIL-100(Al); ■, MIL-100(Fe)_F1; □, MIL-100(Fe)_F2; ▲, MIL-100(V)_1; △, MIL-100(V)_2.
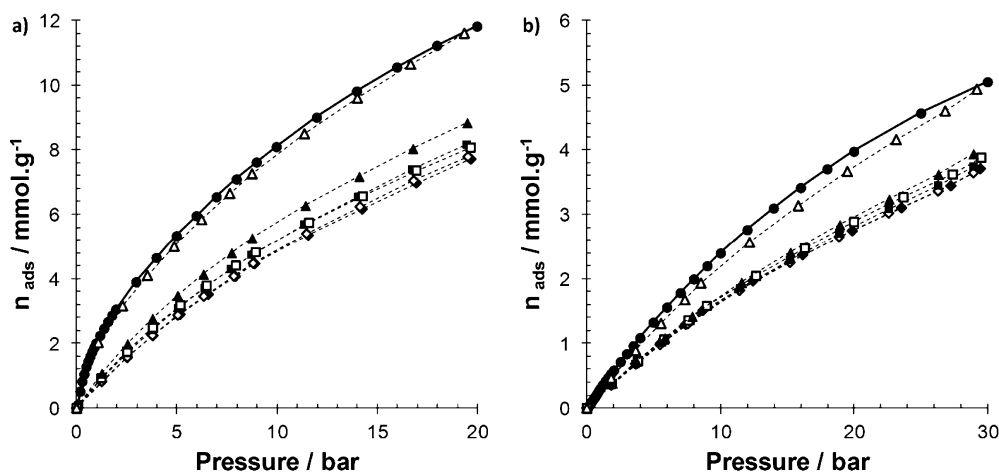

Figure 5. Adsorption isotherms measured at 30 °C for carbon dioxide (a) and methane (b) on MIL-100(Fe)_NF activated at different temperatures using the current apparatus (♦, 30 °C; ◇, 50 °C; ■, 80 °C; □, 110 °C; ▲, 160 °C; △, 250 °C) and activated at 250 °C using a magnetic suspension balance (●).

that for gases which are more strongly adsorbed less sample is required whereas for gases which are only slightly adsorbed, it is recommended to use as much material as possible.

From a practical point of view, for certain types of adsorbents such as MOFs and other materials with similar adsorption mechanisms it is possible to estimate the minimum equivalent BET surface area required to get accurate results. Previous studies[27,28] have shown that at intermediate pressures, the adsorption on MOFs of gases with relatively weak interactions, such as methane, correlates with the apparent BET surface area. Assuming that nitrogen has a similar behavior to methane, one can estimate that a surface of approximately 70 m², the equivalent BET surface of 60 mg of Takeda-5A, is recommended to have sufficiently accurate results for N_2, the least adsorbed of all the gases tested so far. It follows that for materials which have low surface areas, a larger amount of sample is required.

Screening of Adsorbents: MIL-100. Having established the reliability of the apparatus, it was used to evaluate a series of MIL-100 solids synthesized by various routes and with different metals for their gas adsorption properties, using approximately 60 mg of material. Adsorption isotherms for CO_2 and C_3H_6 are

presented in Figure 4 while the CH_4 and C_3H_8 isotherms can be found in the Supporting Information.

In Figure 4a and b, the difference between the two MIL-100(V) samples is related to a small difference in the synthesis conditions, which leads to a slightly lower crystallinity in the MIL-100(V)_1 sample. This explains the systematically lower amounts adsorbed and will be discussed in a little more detail later. Looking at the other materials, it is noticeable that at high pressures the solid with the largest pore volume (MIL-100(Fe)_F2, 0.99 cm³·g⁻¹) also has the highest uptakes while the solid with the smallest pore volume (MIL-100(Al), 0.76 cm³·g⁻¹) adsorbs the least. The isotherms obtained with MIL-100(Fe)_F1 are all very close to those obtained with the F2 sample but with a slightly lower capacity, which is consistent with the lower pore volume (0.85 cm³·g⁻¹). The difference in pore volume between these two samples comes from the additional purification step using NH_4F used in the preparation of MIL-100(Fe)_F2.

The results obtained with MIL-100(Cr) and MIL-100(V)_2 are less easily explained simply based on the BET surface and pore volume. MIL-100(V)_2 has a similar pore volume to MIL-100(Fe)_F1 yet adsorbs systematically less while MIL-100(Cr) has a lower surface area and pore volume than MIL-100(V)_2
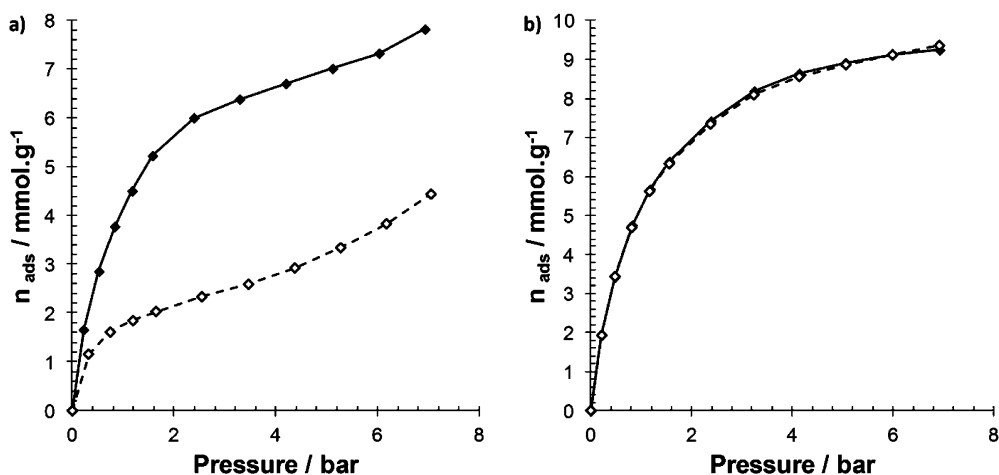
Figure 6. Two adsorption isotherms for propylene on MIL-100(V)_1 (a) and MIL-100(V)_2 (b) measured at 30 °C with a two hour vacuum between cycles. ◆, cycle 1; ◇, cycle 2.

but initially adsorbs as much as MIL-100(Fe)_F1. This is related to the strength of the initial loading sites. MIL-100 is known to have unsaturated metal sites[24,29−31] which directly affect the adsorption at low loadings, especially for CO_2 and propylene. Looking at the first adsorption point for CO_2, it is clear that both MIL-100(Fe)_F samples as well as MIL-100(Cr) have a stronger initial uptake. While in theory Al^{3+} cations have a higher polarizing power than their Cr or Fe counterparts, the use of HF in the synthesis of the MIL-100(Fe)_F and MIL-100(Cr) solids leads to the presence of electron withdrawing F^-ions in the local environment of the Cr^{3+} and the $Fe^{3+/2+}$ sites, which increases their acidity and explains the higher initial uptakes. Thereafter, the isotherms for MIL-100(Fe)_F1 and MIL-100(V)_2 are virtually parallel, consistent with their similar physical characteristics, while MIL-100(Cr) on the other hand has a shallower slope and gradually falls back, again in agreement with its lower surface area and smaller pore volume.

Without going into any more detail, it is clear that the most interesting adsorbent from this series in terms of gas uptake is the MIL-100(Fe)_F2 solid. However, the presence of F in an adsorbent is liable to cause problems in an industrial process, therefore an alternative synthesis route has been developed to produce MIL-100(Fe)_NF.[22]

Optimization of Thermal Activation. Another feature of the apparatus presented here is the ability to activate each sample in situ at a different temperature, which can be used to help determine the optimal activation temperature for new adsorbents. Figure 5 shows adsorption isotherms for carbon dioxide and methane measured at 30 °C on samples (100 mg) of MIL-100(Fe)_NF activated at 30, 50, 80, 110, 160, and 250 °C using the high-throughput apparatus, along with an isotherm measured gravimetrically on a sample activated at 250 °C.

First one can note again the good agreement between the results obtained using the high-throughput apparatus and the magnetic suspension balance for the two samples activated at 250 °C. Second, one can observe the substantial increase in amounts of both CO_2 and CH_4 adsorbed after activation at 250 °C compared to the other temperatures. This corresponds to the removal of a large amount of impurities in the solid between 180 and 200 °C, possibly inorganic impurities such as nitrate and ammonium ions resulting from the synthesis and

activation procedures, which can also be observed by thermogravimetric analysis (see Supporting Information). Interestingly, the amounts of methane adsorbed by the samples activated at all the other temperatures are virtually the same, with the slight spread at high pressures simply due to the very marginally increasing loss in mass during activation, whereas for carbon dioxide there are three clearly distinct isotherms, indicating that between 50 and 80 °C, and again between 110 and 160 °C, there are a small number of CO_2-specific adsorption sites that are made available.

Estimation of Isotherm Reversibility/"Sample Regenerability". The ability to cycle adsorption experiments is essential when evaluating adsorbents for potential separation applications, especially for PSA-type processes. Whether the adsorbed species can be desorbed and the adsorption bed regenerated without incurring unnecessary additional costs is at least as important if not more so than the capacity and selectivity of the material. In our case it is also important to know if the sample has been fully regenerated because the apparatus is designed to measure up to four gases sequentially, therefore any remaining adsorbed species would contaminate experiments with subsequent gases. Figure 6 shows two adsorption isotherms for propylene on the two MIL-100(V) solids mentioned earlier.

As previously mentioned, the difference between the two samples is related to a slight modification of the synthesis conditions which gives the MIL-100(V)_1 (left) material a slightly lower surface area, pore volume, and crystallinity. Consequently, this sample has a lower adsorption capacity than the MIL-100(V)_2 sample for all gases. In addition to this, in the case of propylene adsorption, the second adsorption run gives very different results from the first. While for MIL-100(V)_2 two hours under vacuum was sufficient to fully regenerate the sample, for MIL-100(V)_1 a large amount of adsorbed propylene could not be removed by simple vacuum. This suggests that the adsorption mechanism is not the same and there is most likely some form of chemisorption on very strong adsorption sites, possibly defects in the material. This illustrates the possibility of using the current apparatus not only to evaluate the regenerability of adsorbents but also to highlight differences in the quality of materials obtained by different synthesis routes.
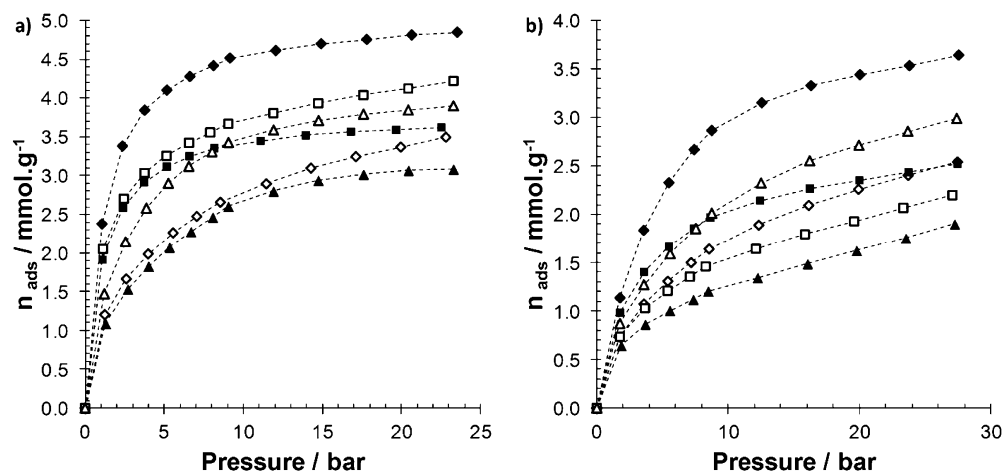
Figure 7. Adsorption isotherms for carbon dioxide (a) and methane (b) on various CAU-10 materials measured at 30 °C. ♦, CAU-10-H; ◇, CAU-10-OH; ■, CAU-10-NH$_2$; □, CAU-10-NO$_2$; ▲, CAU-10-OCH$_3$; △, CAU-10-CH$_3$.

Screening of Adsorbents and Following the Effect of Ligand Substitution: CAU-10. As mentioned earlier, MOFs are a fascinating class of porous material because of the possibility to use many different metals and organic linkers. The effect of varying the metal center has already been presented, here the high-throughput apparatus has been used to study the impact of functionalizing the organic linker in a series of CAU-10 solids. The functional groups (−OH, -NH$_2$, -NO$_2$, -OCH$_3$ and −CH$_3$) serve to alter the surface chemistry of the adsorbent but they also have a non-negligible effect on the diameter of the narrow openings in the pore channels as well as on the accessible surface area and pore volume of the material . For this reason they affect not only the strength of interaction with the adsorbed gases but also the total capacity, as can be seen in Figure 7.

Carbon dioxide (a) and methane (b) adsorption isotherms were measured on 80 mg samples of the various functionalized solids. Although for four of the functionalized materials (−OH, −NH$_2$, −OCH$_3$, and −CH$_3$) no adsorption of N$_2$ at 77 K could be measured, all the samples adsorb both CO$_2$ and CH$_4$ at 303 K. This has been attributed to the increased mobility of the functional groups at the higher temperature, which block the entrance to the channels at 77 K.[20] The order of the CO$_2$ isotherms at the first measurement point is the same as that reported by Reinsch et al., who measured low pressure CO$_2$ adsorption data, and the amounts adsorbed are also in good agreement.

These materials differ from the series of MIL-100 solids presented earlier in that at 20 bar, they are already reaching saturation for CO$_2$; therefore pore volume is critical for the adsorption capacity. As such, it is not surprising that the unmodified solid, which would be expected to have the highest pore volume, also has the highest amounts adsorbed for both CO$_2$ and CH$_4$, and that functionalizing with the bulky −OCH$_3$ group gives the lowest uptakes. Interestingly the −NO$_2$ functionalized material, which also has a fairly bulky functional group, has the second highest CO$_2$ uptake while its methane isotherm is similar to that of CAU-10-OCH$_3$. The increased adsorption of CO$_2$ takes place primarily at initial loading and can be explained by the enhanced interaction of the gas molecules with the functional group. Another interesting observation is the crossing of the -NH$_2$ and −CH$_3$ isotherms at approximately 10 bar. Again, this is probably due to increased

interaction between the gas molecules and the amine group at low loadings, while at higher pressure the larger free-space of the −CH$_3$ functionalized solid leads to higher uptakes. This effect is stronger for the quadrupolar CO$_2$ than for the relatively neutral CH$_4$.

Estimation of Adsorbent Selectivity. Having measured CO$_2$ and CH$_4$ adsorption isotherms on the different functionalized forms of CAU-10, it is then possible to estimate the CO$_2$/CH$_4$ selectivity of these materials using predictive models such as the Ideal Adsorbed Solution Theory.[32] The pure component isotherms were fitted using a Triple Site Langmuir equation (see Table 2 in the Supporting Infomormation for fitted parameters) and the CO$_2$/CH$_4$ selectivity was calculated for an equimolar mixture at 1 and 10 bar (see Table 2), which are potential regeneration and production pressures respectively for a PSA process.

Table 2. Predicted CO$_2$/CH$_4$ Selectivity for a 50% CO$_2$, 50% CH$_4$ Mixture at 1 and 10 bar

adsorbent	selectivity at 1 bar	selectivity at 10 bar
CAU-10-H	4.9	5.8
CAU-10-OH	3.5	3.6
CAU-10-NH$_2$	4.4	6.6
CAU-10-NO$_2$	8.0	13.8
CAU-10-OCH$_3$	1.7	3.5
CAU-10-CH$_3$	3.0	3.6

As expected from the isotherms of the pure gases, all the samples are selective toward CO$_2$. The unmodified material has a selectivity of approximately 5, which is slightly higher than that of an activated carbon,[33] however given its low adsorption capacity it is unlikely to be of interest for a CO$_2$/CH$_4$ separation process. Based in Table 2, two types of functional groups can be distinguished: those that increase the CO$_2$ selectivity (−NH$_2$, −NO$_2$), and those that decrease the selectivity (−OH, −CH$_3$, −OCH$_3$). The increased interaction between CO$_2$ and amine groups is well-known and has been widely investigated;[34−37] however, its effect here appears to be minimal and in fact only apparent at the higher pressure. In the case of the −NO$_2$ modified solid, as previously observed the interaction with CO$_2$ is significantly stronger and this is highlighted by the increased selectivity which is almost double that of the unmodified material. It should be noted however
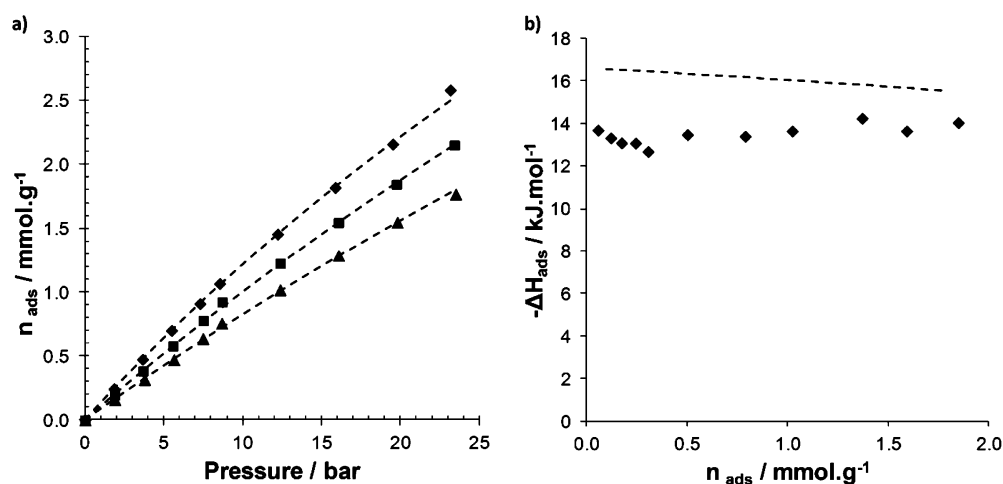
Figure 8. (a) Nitrogen adsorption isotherms measured at 20 °C (♦), 30 °C (■), and 40 °C (▲) on MIL-100(Fe)_F2: symbols = experimental points, dashed lines = fit using Langmuir equation; (b) Comparison between adsorption enthalpies measured by microcalorimetry (♦) and isosteric heats calculated using the Clausius−Clapeyron equation (dashed line) for nitrogen adsorption on MIL-100(Fe)_F2.

that these are only initial estimates for the selectivities and additional experiments either of coadsorption or more precise measurements for the pure gases are required before drawing any more detailed conclusions.

Calculation of Isosteric Enthalpies and Comparison with Direct Calorimetry Measurements. Although the majority of the experiments carried out so far have been measured at 30 °C, the apparatus has been designed to also be able to operate at other temperatures and this allows the possibility of estimating isosteric heats of adsorption using the Clausius−Clapeyron equation. An example of this is presented in Figure 8.

Adsorption isotherms for N_2 on MIL-100(Fe)_F2 were measured at 20, 30, and 40 °C and fitted with a simple Langmuir equation. The calculated isosteric heats are compared with the experimental adsorption enthalpies measured by microcalorimetry (see Supporting Information for more details). The calculated values overestimate the experimental enthalpies by 2−3 kJ·mol^{-1} however it is likely that this could be improved by increasing the number of different temperatures at which isotherms are measured. In any case, the results are close enough to be used as an initial estimate of the heats of adsorption.

CONCLUSION

We have presented here a new high-throughput adsorption instrument capable of rapidly and reliably measuring adsorption isotherms on six samples in parallel using minimal amounts of adsorbent. The experiments can be cycled and up to four different gases can be measured sequentially without any intervention from the operator, meaning that as many as 24 distinct isotherms can be measured in as little as 24 h, which represents a huge improvement for measurements of this type. As little as 60 mg of adsorbent is sufficient to get reasonably accurate results (≤10% error) while more precise measurements can be obtained using 100−150 mg of sample if desired/available.

Examples have been given of how the instrument can be used to compare gas uptakes in isostructural series of MOFs with different metal centers (MIL-100(M)) or functionalized ligands (CAU-10-X), to determine optimal thermal activation conditions for new adsorbents (MIL-100(Fe)_NF), to investigate

adsorption reversibility and to highlight differences in quality of samples (MIL-100(V)). The resulting isotherms can also be used in conjunction with models such as the IAST or the Clausius−Clapeyron equation to estimate selectivities and heats of adsorption, providing thus all the information required for an initial comparison of adsorbents for a given separation process using parameters such as Rege and Yang's PSA sorbent selection parameter[38] or the recently proposed Adsorbent Performance Indicator.[18]

The instrument is designed to measure adsorption at pressures and temperatures close to those required in an industrial separation process and can handle a wide variety of solids and gases. As such, it is an ideal experimental tool for screening new adsorbents for their storage and separation potential.

ASSOCIATED CONTENT

$\mathcal{S}$ Supporting Information

Synthesis details of MIL-100 samples, additional adsorbent characteristics, details of experimental procedures, additional gas adsorption results, and fitting parameters. This material is available free of charge via the Internet at http://pubs.acs.org.

AUTHOR INFORMATION

Corresponding Author

*Phone: +33 (0)4-13-55-18-28. Fax: +33 (0)4-13-55-18-50. E-mail: Philip.Llewellyn@univ-amu.fr.

Notes

The authors declare no competing financial interest.

■ REFERENCES

(1) Ruthven, D. M. *Principles of Adsorption and Adsorption Processes*; John Wiley and Sons: New York, 1984.

(2) Yang, R. T. *Adsorbent: Fundamentals and Applications*; John Wiley & Sons Inc: New York, 2003.

(3) Llewellyn, P. L.; Horcajada, P.; Maurin, G.; Devic, T.; Rosenbach, N.; Bourrelly, S.; Serre, C.; Vincent, D.; Loera-Serna, S.; Filinchuk, Y.; Ferey, G. Complex adsorption of short linear alkanes in the flexible metal−organic-framework MIL-53(Fe). *J. Am. Chem. Soc.* **2009**, *131*, 13002−13008.

(4) Garrido, J.; Linares-Solano, A.; Martin-Martinez, J. M.; Molina-Sabio, M.; Rodriguez-Reinoso, F.; Torregrosa, R. Use of nitrogen vs. carbon dioxide in the characterization of activated carbons. *Langmuir* **1987**, *3*, 76−81.

(5) Stock, N. High-throughput investigations employing solvothermal syntheses. *Microporous Mesoporous Mater.* **2010**, *129* (3), 287−295.

(6) Stock, N.; Biswas, S. Synthesis of metal−organic frameworks (MOFs): Routes to various MOF Topologies, morphologies, and composites. *Chem. Rev.* **2012**, *112*, 933−969.

(7) Micromeritics ASAP 2420 Accelerated Surface Area and Porosimetry System. http://www.micromeritics.com/Product-Showcase/ASAP-2420.aspx.

(8) Quantachrome Autosorb-6B Surface Area and Pore Size Analyzer. http://www.quantachrome.com/gassorption/autosorb6.html.

(9) Wollmann, P.; Leistner, M.; Stoeck, U.; Gruenker, R.; Gedrich, K.; Klein, N.; Throl, O.; Graehlert, W.; Senkovska, I.; Dreisbach, F.; Kaskel, S. High-throughput screening: speeding up porous materials discovery. *Chem. Commun.* **2011**, *47*, 5151−5153.

(10) Wood, C. D.; Tan, B.; Trewin, A.; Niu, H.; Bradshaw, D.; Rosseinsky, M. J.; Khimyak, Y. Z.; Campbell, N. L.; Kirk, R.; Stoeckel, E.; Cooper, A. I. Hydrogen storage in microporous hypercrosslinked organic polymer networks. *Chem. Mater.* **2007**, *19* (8), 2034−2048.

(11) Han, S.; Huang, Y.; Watanabe, T.; Dai, Y.; Walton, K. S.; Nair, S.; Sholl, D. S.; Meredith, J. C. High-throughput screening of metal-organic frameworks for CO2 Separation. *ACS Comb. Sci.* **2012**, *14*, 263−267.

(12) Dueren, T.; Bae, Y.-S.; Snurr, R. Q. Using molecular simulation to characterise metal−organic frameworks for adsorption applications. *Chem. Soc. Rev.* **2009**, *38*, 1237−1247.

(13) Atci, E.; Erucar, I.; Keskin, S. Adsorption and transport of CH_4, CO_2, H_2 mixtures in a Bio-MOF material from molecular simulations. *J. Phys. Chem. C* **2011**, *115*, 6833−6840.

(14) Krishna, R.; van Baten, J. M. In silico screening of metal-organic frameworks in separation applications. *Phys. Chem. Chem. Phys.* **2011**, *13*, 10593−10616.

(15) Kim, J.; Lin, L.-C.; Martin, R. L.; Swisher, J. A.; Haranczyk, M.; Smit, B. Large-scale computational screening of zeolites for ethane/ethene separation. *Langmuir* **2012**, *28*, 11914−11919.

(16) Lin, L.-C.; Berger, A. H.; Martin, R. L.; Kim, J.; Swisher, J. A.; Jariwala, K.; Rycroft, C. H.; Bhown, A. S.; Deem, M. W.; Haranczyk, M.; Smit, B. In silico screening of carbon-capture materials. *Nat. Mater.* **2012**, *11*, 633−641.

(17) Keskin, S.; Sholl, D. S. Efficient methods for screening of metal organic framework membranes for gas separations using atomically detailed models. *Langmuir* **2009**, *25*, 11786−11795.

(18) Wiersum, A. D.; Chang, J.-S.; Serre, C.; Llewellyn, P. L. An adsorbent performance indicator as a first step evaluation of novel sorbents for gas separations: application to metal organic frameworks. *Langmuir* **2013**, submitted.

(19) Ferey, G.; Serre, C.; Mellot-Draznieks, C.; Millange, F.; Surble, S.; Dutour, J.; Margiolaki, I. Molecular modeling: A hybrid solid with giant pores prepared by a combination of targeted chemistry, simulation, and powder diffraction. *Angew. Chem., Int. Ed.* **2004**, *43*, 6296−6301.

(20) Reinsch, H.; van der Veen, M. A.; Gil, B.; Marszalek, B.; Verbiest, T.; De, V. D. E.; Stock, N. Structures, sorption characteristics and nonlinear optical properties of a new series of highly stable aluminium MOFs. *Chem. Mater.* **2012**, DOI: 10.1021/cm3025445.

(21) Horcajada, P.; Surble, S.; Serre, C.; Hong, D.-Y.; Seo, Y.-K.; Chang, J.-S.; Greneche, J.-M.; Margiolaki, I.; Ferey, G. Synthesis and catalytic properties of MIL-100(Fe), an iron(III) carboxylate with large pores. *Chem. Commun.* **2007**, 2820−2822.

(22) Seo, Y.-K.; Yoon, J. W.; Lee, J. S.; Lee, U. H.; Hwang, Y. K.; Jun, C.-H.; Horcajada, P.; Serre, C.; Chang, J.-S. Large scale fluorine-free synthesis of hierarchically porous iron(III) trimesate MIL-100(Fe) with a zeolite MTN topology. *Microporous Mesoporous Mater.* **2012**, *157*, 137−145.

(23) Volkringer, C.; Popov, D.; Loiseau, T.; Ferey, G.; Burghammer, M.; Riekel, C.; Haouas, M.; Taulelle, F. Synthesis, single-crystal X-ray microdiffraction, and NMR characterizations of the giant pore metal−organic framework aluminum trimesate MIL-100. *Chem. Mater.* **2009**, *21*, 5695−5697.

(24) Lieb, A.; Leclerc, H.; Devic, T.; Serre, C.; Margiolaki, I.; Mahjoubi, F.; Lee, J. S.; Vimont, A.; Daturi, M.; Chang, J.-S. MIL-100(V)—A mesoporous vanadium metal organic framework with accessible metal sites. *Microporous Mesoporous Mater.* **2012**, *157*, 18−23.

(25) Lemmon, E. W.; McLinden, H. M. *MO Reference Fluid Thermodynamic and Transport Properties*; REFPROP 8.0; National Institute of Standards and Technology: Gaithersburg, MD, 2007.

(26) *GUM 1995 with Minor Corrections*; Joint Committee for Guides in Metrology: France, 2008.

(27) Dueren, T.; Sarkisov, L.; Yaghi, O. M.; Snurr, R. Q. Design of new materials for methane storage. *Langmuir* **2004**, *20*, 2683−2689.

(28) Frost, H.; Dueren, T.; Snurr, R. Q. Effects of surface area, free volume, and heat of adsorption on hydrogen uptake in metal−organic frameworks. *J. Phys. Chem. B* **2006**, *110*, 9565−9570.

(29) Llewellyn, P. L.; Bourrelly, S.; Serre, C.; Vimont, A.; Daturi, M.; Hamon, L.; De, W. G.; Chang, J.-S.; Hong, D.-Y.; Hwang, Y. K.; Jhung, S. H.; Ferey, G. High uptakes of CO_2 and CH_4 in mesoporous metal−organic frameworks MIL-100 and MIL-101. *Langmuir* **2008**, *24*, 7245−7250.

(30) Yoon, J. W.; Seo, Y.-K.; Hwang, Y. K.; Chang, J.-S.; Leclerc, H.; Wuttke, S.; Bazin, P.; Vimont, A.; Daturi, M.; Bloch, E.; Llewellyn, P. L.; Serre, C.; Horcajada, P.; Greneche, J.-M.; Rodrigues, A. E.; Ferey, G. Controlled reducibility of a metal−organic framework with coordinatively unsaturated sites for preferential gas sorption. *Angew. Chem., Int. Ed.* **2010**, *49*, 5949−5952.

(31) Volkringer, C.; Leclerc, H.; Lavalley, J.-C.; Loiseau, T.; Ferey, G.; Daturi, M.; Vimont, A. Infrared spectroscopy investigation of the acid sites in the metal−organic framework aluminum trimesate MIL-100(Al). *J. Phys. Chem. C* **2012**, *116*, 5710−5719.

(32) Myers, A. L.; Prausnitz, J. M. Thermodynamics of mixed-gas adsorption. *AIChE J.* **1965**, *11*, 121−7.

(33) Sircar, S.; Golden, T. C.; Rao, M. B. Activated-carbon for gas separation and storage. *Carbon* **1996**, *34*, 1−12.

(34) Arstad, B.; Fjellvaag, H.; Kongshaug, K. O.; Swang, O.; Blom, R. Amine functionalised metal organic frameworks (MOFs) as adsorbents for carbon dioxide. *Adsorption* **2008**, *14*, 755−762.

(35) Vitillo, J. G.; Savonnet, M.; Ricchiardi, G.; Bordiga, S. Tailoring metal−organic frameworks for CO_2 capture: The amino effect. *ChemSusChem* **2011**, *4*, 1281−1290.

(36) Yang, Q.; Wiersum, A. D.; Llewellyn, P. L.; Guillerm, V.; Serre, C.; Maurin, G. Functionalizing porous zirconium terephthalate UiO-66(Zr) for natural gas upgrading based on a computational exploration. *Chem. Commun.* **2011**, *47*, 9603−9605.

(37) Yuan, B.; Ma, D.; Wang, X.; Li, Z.; Li, Y.; Liu, H.; He, D. A microporous, moisture-stable, and amine-functionalized metal−organic framework for highly selective separation of CO_2 from CH_4. *Chem. Commun.* **2012**, *48*, 1135−1137.

(38) Rege, S. U.; Yang, R. T. A simple parameter for selecting an adsorbent for gas separation by pressure swing adsorption. *Sep. Sci. Technol.* **2001**, *36*, 3355−3365.